JOURNAL OF PROPULSION AND POWER
Vol. 15, No. 3, May–June 1999

Modified Through-Flow Wave-Rotor Cycle with Combustor-Bypass Ducts

Daniel E. Paxson*
NASA John H. Glenn Research Center at Lewis Field, Cleveland, Ohio 44135
and
M. Razi Nalim†
Indiana University–Purdue University at Indianapolis, Indianapolis, Indiana 46202

A wave-rotor cycle is described that avoids the inherent problem of combustor exhaust gas recirculation (EGR) found in four-port, through-flow (uniflow) pressure-gain wave-rotor cycles currently under consideration for topping gas-turbine engines. The recirculated hot gas is eliminated by the judicious placement of a bypass duct that transfers gas from one end of the rotor to the other. The resulting cycle, when analyzed numerically, yields a mean absolute temperature for the rotor that is 18% below the already impressive value (approximately the turbine inlet temperature) predicted for the conventional four-port cycle. The absolute temperature of the gas leading to the combustor is also reduced from the conventional design by 17%. The overall design-point pressure ratio of this new bypass cycle is approximately the same as the conventional cycle. This paper will describe the EGR problem and the bypass-cycle solution, including relevant wave diagrams. Performance estimates of design and off-design operation of a specific wave rotor will be presented. The results were obtained using a one-dimensional numerical simulation and design code.

Nomenclature

g_c = Newton constant
L = length of rotor
$\dot{m}$ = mass flow rate
p = pressure
$\dot{Q}$ = heat addition rate
R = gas constant
T = temperature
t = time
x = axial position
γ = specific heat ratio

Subscripts

c = corrected
wall = rotor passage wall
0 = stagnation state
01 = inlet stagnation state
04 = exhaust stagnation state
1 = inlet
4 = exhaust

Introduction

PRESSURE-GAIN wave rotors represent a promising technology for use as high-pressure, high-temperature topping cycles in gas-turbine engines.[1–3] Among their potential advantages are rotor metal temperatures substantially below the combustor-discharge temperature, rotational speeds that are approximately one-third those of conventional turbomachinery, a wide operating range,[4] and relatively simple rotor geometry. Recent research efforts have focused largely on four-port, through-flow, pressure-gain cycles with axially aligned passages of uniform cross section. This design, shown schematically in Fig. 1, is attractive in that it is relatively easily integrated into existing gas-turbine engines as another spool.[5] While the transition ducts between partial and full annular flows are often a design challenge, past designs using reverse-flow and symmetrical-flow cycles exacerbated this issue.

The terms through-flow or uniflow refer to the general tendency for all of the flow entering the wave rotor to completely traverse the passage before exiting. In other words, the flow comes in one end and goes out the other. In contrast, reverse-flow cycles draw gas through one port and discharge it through another at the same end of the rotor. For example, with reference to Fig. 1, air enters through port 1 but, in a reverse-flow cycle, is sent to the combustor through a port located in the place of port 3. Each gas stream entering the passages thus tends to remain closer to one end of the rotor. Symmetrical-flow rotors have an even number of alternating cycles that are mirror images of each other, requiring each type of port to be placed at alternating ends of the rotor.

In principle, through-flow designs take best advantage of the self-cooling capabilities of wave rotors because each passage is washed by hot and cold gas passing alternately over its entire length. The short time scale of this temperature variation relative to the thermal response time of the rotor wall implies that a time-mean temperature profile will be established in the wall, which depends on the cycle and on wall conductivity. Estimates of the rotor-wall temperature in a conventional through-flow wave rotor, designed for an overall stagnation temperature ratio (T_{04}/T_{01} in Fig. 1) of ~2.2, indicate that it is relatively uniform along the entire passage and roughly equal to the downstream turbine inlet temperature. For most wave-rotor designs, this is 20–25% below the combustor-exit absolute temperature. In a representative application to a small gas-turbine engine, this amounts to a 660°F (367°C) difference between rotor-wall and combustor-exit temperature. This estimate was made using a one-dimensional computational fluid dynamics (CFD) code developed specifically for wave-rotor analysis.[4] The port conditions predicted by the code have been validated using data from several wave-rotor experiments.[6]

Presented as Paper 97-3140 at the AIAA/ASME/SAE/ASEE 33rd Joint Propulsion Conference, Seattle, WA, July 6–9, 1997; received Dec. 4, 1997; revision received Nov. 17, 1998; accepted for publication Nov. 19, 1998.

*Aerospace Engineer, Controls and Dynamics Technology Branch, M/S 77-1. Member AIAA.
†Assistant Professor, Purdue School of Engineering and Technology, Mechanical Engineering, SL 260. Senior Member AIAA.

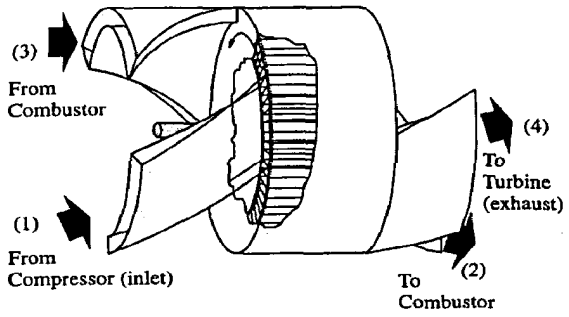

Fig. 1 Generic four-port, through-flow wave rotor.

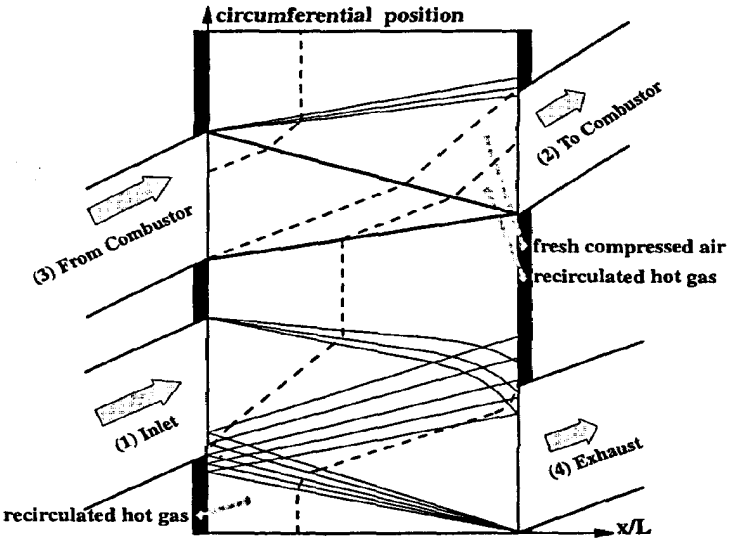

Fig. 2 Wave diagram of the conventional, four-port, through-flow wave-rotor cycle at the design point.

While this is an impressive degree of cooling, in many engine-topping applications, the rotor temperatures would still be unacceptable for a rotor composed of conventional materials. This cooling limitation is related to the fact that a pressure-gain wave rotor with equal mass flows in the inlet and exhaust cannot contain, in passages of equal volume, equal masses of relatively hotter and colder gases at different times. Consequently, each passage is only partially filled with fresh air in each cycle, and only partially exhausted of hot gas. Furthermore, this results in the conventional through-flow design containing a gas path in which the flow going to the combustor is a mixture of both fresh compressed air and recirculated hot gas from the combustor. This is illustrated in Fig. 2, which shows a simplified wave diagram for the rotor passage as it rotates through a complete wave cycle, i.e., an x–t diagram, where t represents either time or circumferential position of a rotor passage. The solid lines in the figure represent the trajectories of selected wave fronts. The dashed lines represent selected particle paths. At the top and bottom of the wave diagram, the passage is filled completely with hot combustion gas entering the rotor from port 3. Only a part of this hot gas is discharged through exhaust port (4), leading to the downstream turbine, indicated by a particle path for the last discharged particle. As such, when a passage reaches port (2), leading to the combustor, the remaining hot gas is discharged first, followed by the compressed fresh air brought onboard from the inlet duct (port 1). Because of compression, the discharged hot gas is locally even hotter than the combustor exit temperature (port 3), and it presents a challenge in designing the initial portion of the duct receiving it. These hot and cold gases generally mix in the duct, and the resulting flow can be still too hot to cool the combustor liner.

This paper will describe a new through-flow cycle that overcomes the exhaust gas recirculation problem by using a simple, strategically placed, bypass duct. The duct transfers some of the working fluid (air) from one end of the wave rotor to the other, bypassing the combustor. The resulting cycle, after some repositioning of port locations and adjustment of the rotor speed to ensure proper wave timing, replaces what was once hot combustor-exhaust gas in the wave-rotor passage with cooler reinjected air. This, in turn, yields a rotor with a lower mean wall temperature, equivalent performance, and only relatively cold air going to the combustor. Details of the new design will be presented. Numerical performance estimates will be shown and compared with a conventional, four-port, through-flow design sized for the same mass flow rate and the same overall temperature ratio. Estimated wall temperatures and combustor inlet temperatures will be compared. Finally, potential technical challenges associated with this cycle will be discussed.

The results presented in this paper were obtained using a numerical wave-rotor simulation that has been well documented in the literature.[4,6] The paper relies heavily on the reader's familiarity with the wave-rotor operating principles, which will not be presented here. Excellent descriptions can be found elsewhere in the literature,[7,8] and a short list of descriptive sources can be found in Ref. 9.

Bypass Cycle Description

The basic version of the new cycle is illustrated in Fig. 3, which, in the manner of Fig. 2, is a wave diagram for a complete wave cycle. Fresh air enters the rotor through port 1 and is compressed by a series of shock and compression waves. Most or all of this compressed air then exits the rotor via the port leading to the bypass duct, which is separated from port 2 by a thin splitter plate. Depending on design conditions, some fresh air may be split away through port 2 leading to the combustor. Compressed air in the bypass duct is then routed to the other end of the rotor and reinjected via a duct located just aft of the hot-gas duct coming from the combustor (port 3). This air is then expanded, along with the hot gas that came from the combustor, by the strong expansion wave generated by the opening of port 4. The accompanying outflow process purges the hot gas from the wave-rotor passage, but leaves the reinjected bypass air onboard. With the subsequent compression wave process, the reinjected air is now sent to the combustor through port 2 along with some fresh compressed air. This air is then heated in the combustor and returned to the rotor through port 3. The preceding version of the bypass cycle will be referred to as the separated-bypass cycle. Note that the amount of gas going to the bypass loop is adjustable in the design process, during which port positions and rotor speed are matched to the gasdynamics, and conservation laws are enforced. That is, cycles may be designed such that some exhaust gas recirculation (EGR) still exists, though not as much as shown in Fig. 2. The particular cycle shown in Fig. 3 represents the elimination of EGR,

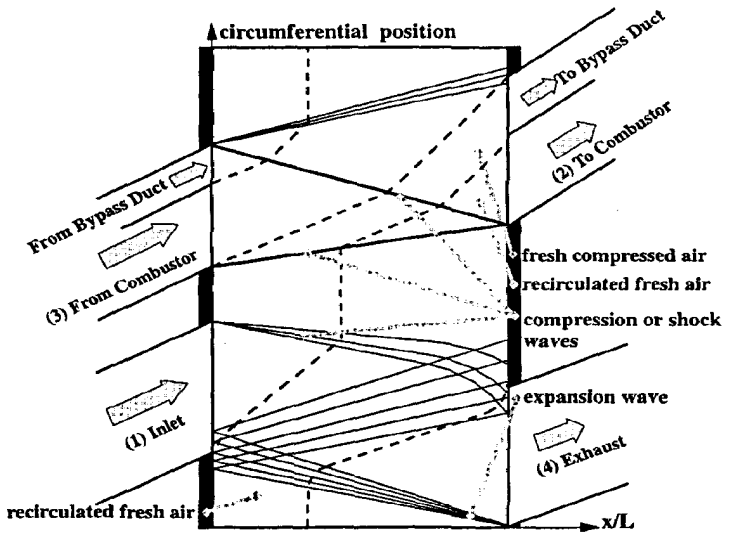

Fig. 3 Wave diagram of the through-flow, bypass wave-rotor cycle at the design point.

Table 1 Post stagnation conditions[a]

Bypass (Conventional)	p_0/p_{01}	T_0/T_{01}	$\dot{m}/\dot{m}_1$
Port 2	3.462	1.692	1.000
	(3.257)	(2.038)	(1.540)
Port 3	3.078	2.900	1.000
	(2.972)	(2.821)	(1.540)
Port 4	1.221	2.209	1.000
	(1.203)	(2.208)	(1.000)
Port to bypass	3.418	1.504	0.925
Port from bypass	3.177	1.504	0.925

[a]At the design point of conventional and bypass through-flow wave rotors sized for 4.8-lbm/s mass flow rate.

Table 2 Post stagnation conditions[a]

Simplified bypass (Separated bypass)	p_0/p_{01}	T_0/T_{01}	$\dot{m}/\dot{m}_1$
Port 2	3.433	1.669	1.840
	(3.462)	(1.692)	(1.000)
Port 3	3.057	2.876	1.000
	(3.078)	(2.900)	(1.000)
Port 4	1.231	2.201	1.000
	(1.221)	(2.209)	(1.000)
Port to bypass	3.418	1.504	0.925
Port from bypass	3.144	1.669	0.840
	(3.177)	(1.504)	(0.925)

[a]At the design point of separated and simplified bypass wave-rotor cycles sized for 4.8-lbm/s mass flow rate.

or alternately, the maximum useful cold bypass flow. Therefore, all of the hot combustion gas entering at port 3 leaves the passage through port 4 immediately. The cycle design process is similar to that described in Ref. 3 and will not be presented here. Off-design behavior is discussed later.

Comparing Figs. 2 and 3, several salient features may be observed. First, that portion of the passage which, in the conventional cycle, is filled with hot recirculated gas from the combustor is now occupied by relatively cool air from the bypass loop. This is the primary mechanism leading to improved rotor cooling. Second, all of the flow going to the combustor is relatively cool air. The nonsteady flows and the performance of the wave rotor were computed for this separated-bypass cycle and for the conventional cycle, for a particular 4.8-lbm/s wave rotor described in the section labeled Overall Performance. Table 1 lists the mixed, i.e., averaged over the width of the port, stagnation pressure and temperature, and the mass flow rate in each port, relative to the inlet state, for both cycles. The gas (substantially air) in port 2 of the bypass cycle is 17% cooler than that in the conventional cycle.

It may appear from Fig. 3 that the gas paths allow for a clear distinction between the wave compressor and wave turbine components of the cycle. As such, the information from Table 1 could be used to calculate component efficiencies (adiabatic or polytropic). Such calculations would not be meaningful for several reasons. First, there is significant heat transfer from the rotor walls to the relatively cool air, and from the hot gas to the rotor walls. The heat transfer leads to apparent reductions in compression efficiency and increases in expansion efficiency. Second, although the interfaces between hot and cold gases appear sharp in Figs. 2 and 3, in reality this is not the case. The behavior of hot/cold interfaces in a wave rotor is a complex, multidimensional phenomenon.[10,11] Even from an elementary perspective, it is clear that a wave-rotor passage has a finite width, which gives rise to a spreading or smearing of interfaces. The spreading may be compounded when the interface passes through an expansion wave. The general result of interface spreading is that some hot gas can enter ports intended for cold flow, and vice versa. Interface spreading that is a result of the gradual opening and closing of passages of finite width is modeled in the CFD simulation used for this paper. Therefore, these effects are seen in Table 1, and, like the heat transfer phenomena, cause calculated compression efficiencies to appear reduced and expansion efficiencies increased. (Modifications have been made to the boundary conditions of the one-dimensional, CFD wave-rotor model of Refs. 4 and 6 used for this investigation. These now allow computation when the passage is simultaneously partially exposed to more than one port at one end. This occurs, e.g., as the passage moves from port 3 to the port leading from the bypass duct in Fig. 3. These modifications have not been published as of this writing.)

Simplified Bypass

When EGR is almost eliminated, the gas conditions in port 2 and in the port leading to the adjacent bypass duct are relatively close to one another. It may therefore be beneficial to simplify the bypass cycle by eliminating the duct wall that separates them and allow the two gas (air) streams to mix. This configuration is illustrated in Fig. 4. The two streams coming from port 2 are mixed to an

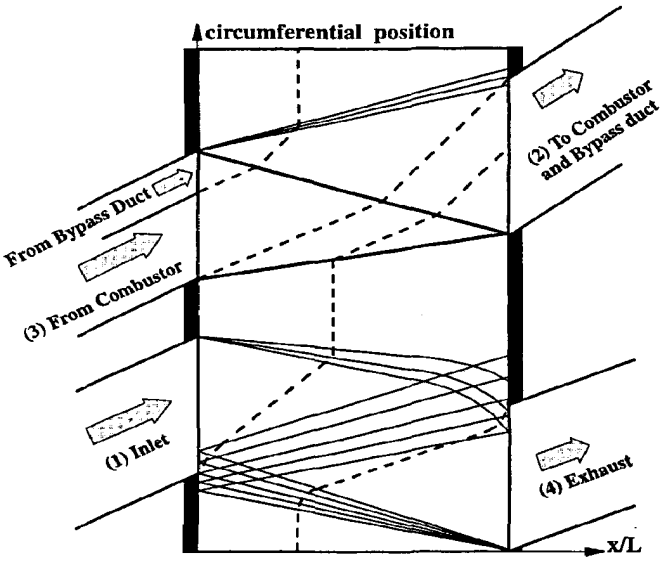

Fig. 4 Wave diagram of the simplified bypass wave-rotor cycle at the design point.

average state (within the simulation this is done using a constant-area mixing calculation[9]), and then split somewhere downstream, prior to the combustor. The air mass flow for the combustor (feeding port 3) is required to match the turbine mass flow (port 4), while the remaining air, still cool but not as fresh, bypasses the combustor for reinjection into the rotor. In this simplified-bypass design, there is only a single high-pressure duct, as in the conventional cycle. The combustor secondary airflow, its liner design, and the bypass airflow are integrated within a single pressure casing. The performance of this cycle is nearly identical to the separated-bypass configuration illustrated in Fig. 3. For reference, the gas states and port mass flow rates at the design point are listed in Table 2, in a manner similar to Table 1, for the separated-bypass and simplified-bypass cycles.

Reverse-Flow Cycle

Although the focus of this paper is primarily on through-flow cycles, it is noted briefly that the bypass modification can be implemented in a reverse-flow cycle as well. This is shown in Fig. 5 using the same technique as Figs. 2–4. The rotor dimensions, inlet mass flow rate, and value of overall stagnation temperature ratio, T_{04}/T_{01}, used to design this cycle were the same as those used for Figs. 2–4. The overall stagnation pressure ratio, p_{04}/p_{01}, is the same as the through-flow cycle shown in Fig. 3. Unlike the through-flow cycle, a correctly designed conventional four-port, reverse-flow cycle exhibits no EGR phenomenon. Instead, in a pressure-gain wave rotor with equal mass flows in inlet and exhaust, a mass of gas is perpetually trapped and oscillates within each rotor passage, but never leaves.[1] The composition of this mass at steady state may be a mixture of air and combustion gas depending on port timings and prior transients, but it will become increasingly hot as a result of

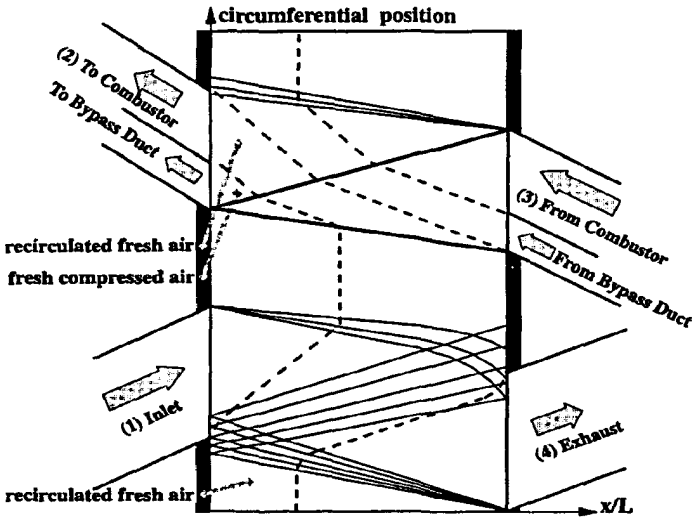

Fig. 5 Wave diagram of the reverse-flow, bypass wave-rotor cycle at the design point.

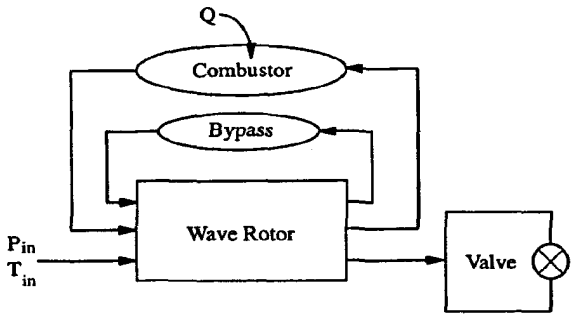

Fig. 6 Simulation schematic.

viscous and shock dissipation until its temperature is limited by heat losses. It is equivalent to the mass that gives rise to EGR in a conventional through-flow cycle, and occurs for the same reason. The bypass reverse-flow cycle eliminates this problem, allowing all of the gas that enters the wave rotor to eventually leave, and reducing the rotor temperature.

Overall Performance

To assess wave-rotor performance realistically, specific flow requirements must be selected. Those selected for this paper were a mass flow rate of 4.8 lbm/s, a ratio of exhaust to inlet temperature (T_{04}/T_{01} in Fig. 1) of 2.2, and inlet conditions corresponding to an upstream compressor pressure ratio of 7.8. A conventional through-flow and a separated-bypass cycle were designed, both using the same rotor geometry and requirements, to allow direct performance comparison. In fact, the rotor geometry, e.g., length, mean radius, number of passages, etc., was taken from a previously published four-port, through-flow design.[4,5] As such, no optimization of the bypass cycle was performed in the manner of Ref. 3; only the port positions and rotor speed were varied to obtain correct wave timing. The conventional and bypass rotors were both designed to be free-wheeling, meaning that there is no independent drive motor. Torque is assumed to be generated by changes in angular momentum as the flow in the inlet ducts is turned from the duct angles to follow the walls of the rotor. Windage effects are neglected in the modeling; however, they are expected to be low for the rotor speeds and geometries of most pressure-gain wave-rotor designs. Friction arising from bearings is also neglected. If the sum of the torque generated by the two (or three) inlet ducts is zero, the rotor speed is constant.

A schematic of the simulation components used to predict the wave-rotor performance is shown in Fig. 6. The components have been documented in Refs. 4 and 6, except for the bypass loop, which is discussed here. The inlet gas state, exhaust valve area, and heat

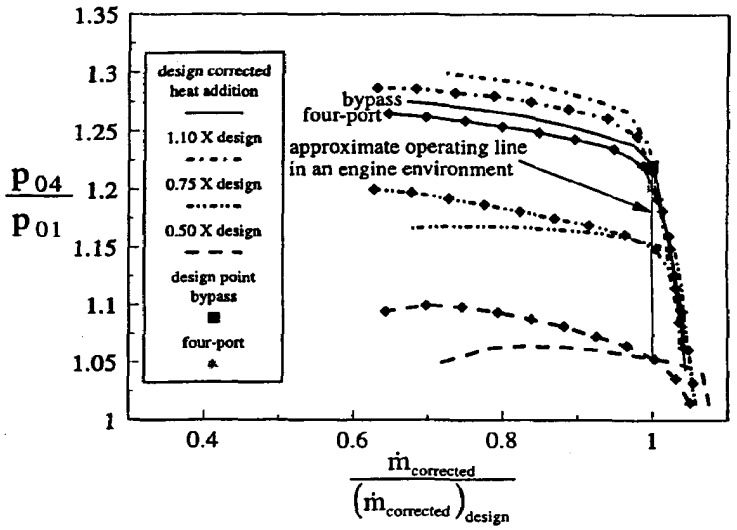

Fig. 7 Performance map for bypass and four-port conventional wave rotors sized for 4.8-lbm/s design-point mass flow rate.

addition rate, i.e., fuel flow rate, were variables. For the performance predictions, the inlet gas state was kept constant at the design-point value.

The separated-bypass and conventional through-flow performance maps are shown in Fig. 7. Each curve on the map was generated using a fixed, specified heat addition rate, whereas the exhaust valve area was varied. The curves without symbols represent the bypass cycle. The curves with symbols represent the four-port conventional cycle. The design operating points for the two cycles are also shown with a dark square symbol representing the bypass cycle and a light gray square representing the four-port conventional cycle. For each point on the map, the exhaust valve area was set and the simulation was run until 1) the sum of the mass flows from all of the wave-rotor ports was zero; 2) the time rates of change for all of the plena, i.e., combustor, bypass, rotor leakage cavity, were zero; and 3) the net torque was zero. The horizontal axis of Fig. 7 is the nondimensional corrected flow rate, which is defined as

$$\dot{m}_c = (\dot{m}/p_{01}A_1)\sqrt{RT_{01}/g_c} \tag{1}$$

where p_{01} and T_{01} are the inlet stagnation pressure and temperature, respectively, A_1 is the inlet cross-sectional area at the rotor face, and R is the gas constant for air. The corrected heat addition rate, which is constant along each curve, is defined as

$$\dot{Q}_c = \dot{Q}/p_{01}A_1\sqrt{RT_{01}g_c} \tag{2}$$

The vertical axis is the ratio of exhaust to inlet stagnation pressure of the wave rotor (see Fig. 1). Because wave-rotor performance is sometimes stated in terms of p_{04}/p_{01} vs T_{04}/T_{01}, the following may be used:

$$\frac{T_{04}}{T_{01}} = 1.0 + \frac{(\gamma - 1)}{\gamma}\frac{\dot{Q}}{\dot{m}_c} \tag{3}$$

Figure 7 also shows an approximate steady-state operating line exhibited by the rotor when it is in the topping cycle environment.[1,4] Typically, the corrected $\dot{Q}_c$ along this line ranges from 1.02 to 0.85 of the design value, representing 100–43% engine power ratings. In Fig. 7, it has been extended down to the value $\dot{Q}_c = 0.50$ of design in order to obtain some indication of performance near idle.[5]

It can be seen from Fig. 7 that the computed performance of the bypass cycle is somewhat better than the conventional design along the entire operating line. The improvement is most likely because the bypass cycle is, fortuitously, a more optimal design. Optimization of topping-cycle wave rotors is discussed in Ref. 3. The present investigation did not focus on optimization, and began with a conventional-cycle design that had a rotor speed slightly

higher than optimal because of an emphasis on minimizing leakage, but was otherwise nearly optimal based on past experience. For correct wave timing, the bypass cycle required a lower speed, more nearly optimal, because the cooler temperatures generally slow the waves. The two cycles are expected to perform equivalently when each is optimized, as long as leakage losses can be minimized.

The performance of the bypass cycle appears to drop off more rapidly than the conventional cycle at the lower heat addition rates when the corrected mass flow rate is reduced. Numerical simulations have indicated that operation of the wave rotor in regions where the slopes of the curves in Fig. 7 are positive may lead to instabilities.[4] This observation may mean that the bypass cycle is more susceptible to unstable operation near idle conditions than the conventional cycle; however, it is by no means a definitive conclusion. It should be noted that some regions of this map are disallowed by temperature limitations and the heating value of typical fuels in air, but this constraint was not included.

Rotor Cooling

The rotor-wall temperature is computed simultaneously with the flow, using the heat transfer model of the one-dimensional design code.[4] This model accounts for heat transfer between the passage walls and the internal flow using a semi-empirical correlation analogous to that used to model the momentum transport to the walls (friction).[12] The effect of friction on wave-rotor performance predicted by the model has been experimentally verified.[6] The model also includes heat transfer between the walls and the housing cavities fed by leakage. It is noted that the wall temperature estimates are based on the assumption of radial heat transfer and conduction only, on the top and bottom walls of the passage. These are assumed thermally thin and locally equal in temperature. No account is made for heat conduction in the wall along the passage (in the axial direction), resulting in the worst-case temperature variations and longitudinal thermal gradients. It is acknowledged that a one-dimensional flow model inherently cannot directly compute convective heat transfer in the transverse direction. Nevertheless, it is believed that the predicted relative cooling effect, because of the reinjection of colder bypass air in place of hot combustion gas, is substantially correct.

The computed design-point steady-state distributions of wall temperature along a passage are shown in Fig. 8 for the conventional, separated-bypass, and simplified-bypass cycles (all through-flow), and for the reverse-flow bypass cycle. The wall temperatures have been scaled by the exhaust-port stagnation temperature, T_{04}. It is seen in the figure that all of the bypass cycles are significantly cooler than the conventional cycle, and far below the peak cycle temperature listed for port 3 in Table 1. The average values of the distributions in Fig. 8 are listed in Table 3. Note that, although the reverse-flow bypass cycle yields the lowest mean wall temperature, it is clear from Fig. 8 that there is significant variation from end to end. In contrast, all of the through-flow cycles have relatively uniform temperature distributions.

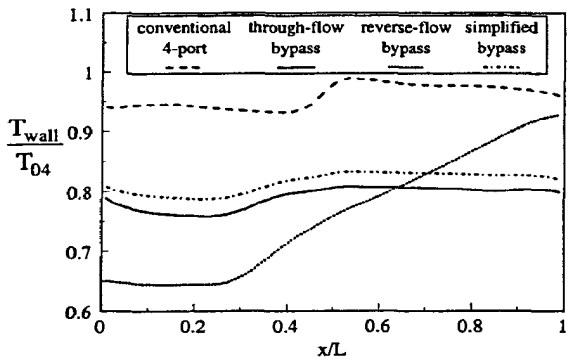

Fig. 8 Design-point wall temperature distributions for a conventional through-flow cycle and several bypass cycles sized for 4.8-lbm/s mass flow rate.

Table 3 Mean design-point rotor-wall temperature estimates[a]

	Conventional four-port	Through-flow bypass	Reverse-flow bypass	Simplified bypass
T_{wall}/T_{04}	0.96	0.79	0.76	0.82

[a]For a conventional cycle and several bypass cycles sized for 4.8-lbm/s mass flow rate.

Discussion

The results presented in the preceding text indicate that the bypass cycle, when compared with the conventional through-flow cycle, provides equal or improved aerodynamic performance throughout the normal operating range, and also significantly reduced temperatures in the rotor, ducting, and combustor. These benefits are substantial. In many applications they may make the difference between a wave rotor that is truly self-cooling, with metal temperatures well within the material limits of conventional construction materials, and one that is merely cooler than the combustor exhaust gas. Nevertheless, it is worthwhile to consider some possible challenges that arise from the bypass design, keeping in mind that such considerations are preliminary. These are outlined next.

Ducting

A separated-bypass design may require more complex ducting compared with the conventional design. It would appear, because the pressures and velocities in the combustor and bypass loop ports are nearly identical, that the two ducts could be continuously joined to one another, separated only by a single wall. For the simplified-bypass cycle, there is only one high-pressure duct as in the conventional cycle, but it is cooler. By definition, however, the bypass flow does not pass through the combustor and must have a separate path around it. This may somewhat complicate the integration of the wave rotor within an existing gas-turbine engine design. Note that the combined volumetric flow rate of combustor and bypass-loop flows in the bypass cycle is nearly identical to the combustor volumetric flow in the conventional cycle. This implies that the volume of ducting in the two designs is comparable.

Combustor Pressure Drop

A difficulty of the bypass cycle is the large combustor pressure drop, $\Delta p_0 = p_{02} - p_{03}$, required to properly balance the wave cycle in the manner shown here. This has also been observed in reverse-flow four-port cycles. Table 1 shows that for the through-flow, conventional cycle the maximum tolerable combustor pressure drop $\Delta p_0/p_{02}$ is 8.8%, whereas for the bypass cycle it is 11.1%. It may be argued that the complex ducting of the wave rotor will incur a larger loss than the usual 3–5% seen on conventional turbomachinery combustor sections. Yet it is difficult to envision a value as large as that allowed for the bypass cycle. Improved design methodologies could take advantage of the lower-than-allowed pressure drops likely in well-designed combustor and bypass flow paths to improve the overall performance of the wave rotor.

Interface Distortion

A third potential issue with the bypass cycle involves the structure of the hot/cold interfaces. Those are the regions of the gas path when hot flow is contiguous with cold, which occur in both the conventional and bypass cycles. They can be seen in Fig. 2 between the compressed air onboard the passage and the gas coming from the combustor, and also between the combustor EGR gas and that coming onboard the rotor from the inlet. In Fig. 3 they are seen between the compressed flow from the inlet and that coming from the combustor, and also between the flow from the combustor and the flow from the bypass duct. It has been observed in multidimensional computations[10] that this interface becomes highly distorted as it traverses the passage, so much so that mass-averaged port pressures and temperatures are different from values computed using one-dimensional models. Whether the interface distortions are worse in the bypass than in the conventional cycle is an issue that requires investigation both computationally and experimentally.

Bleed Flow for Downstream Turbine Cooling

The question of what is the best site on the wave rotor from which to extract cooling flow for downstream turbomachinery is still unanswered. In some applications it may be practical to take this air from the high-pressure regions of the cycle. In the conventional through-flow cycle, this air can only be accessed via strategically positioned taps in the duct leading to the combustor. Furthermore, given the preceding description of interface distortion, it is questionable if the fresh air could be completely isolated from the recirculated hot gas. In the bypass cycle, however, high-pressure air is readily available after it is brought onboard through the duct leading from the bypass loop. A tap located on the end plate could be used to extract the required amount using a relatively weak expansion wave. An alternative coolant-extraction scheme would utilize the region between ports 1 and 3 in Figs. 2 and 3. The bypass cycle then offers no extraction advantage over the conventional cycle, but this scheme may not provide enough air at sufficient delivery pressure.

Conclusions

A new bypass wave-rotor cycle has been described that appears to solve the problems of exhaust gas recirculation and insufficient rotor cooling found in the conventional four-port pressure-gain cycle. Such a cycle has been successfully designed using a one-dimensional numerical simulation. Results from the simulation show that the bypass cycle, when compared with the conventional through-flow cycle, yields an 18% reduction in average rotor-wall temperature, a 17% reduction in combustor inlet temperature, and equivalent or improved overall pressure ratio, p_{04}/p_{01}. The allowed combustor pressure drop is increased from 8.7 to 11.1% for cyclic operation as predicted here, but an improved rotor design may reduce this value. Further experimental and numerical investigation is needed and warranted, given the substantial cooling benefits predicted for the rotor, combustor, and ducting.

References

[1]Welch, G. E., Jones, S. M., and Paxson, D. E., "Wave-Rotor-Enhanced Gas Turbine Engines," *Journal of Engineering for Gas Turbines and Power*, Vol. 119, No. 2, 1997, pp. 469–477; also NASA TM-106998, July 1995.

[2]Jones, S. M., and Welch, G. E., "Performance Benefits for Wave Rotor-Topped Gas Turbine Engines," American Society of Mechanical Engineers, Paper 96-GT-075, June 1996; also NASA TM-107193, June 1996.

[3]Wilson, J., and Paxson, D. E., "Wave Rotor Optimization for Gas Turbine Engine Topping Cycles," *Journal of Propulsion and Power*, Vol. 12, No. 4, 1996, pp. 778–785; also NASA TM-106951, May 1995.

[4]Paxson, D. E., "A Numerical Model for Dynamic Wave Rotor Analysis," *Journal of Propulsion and Power*, Vol. 12, No. 5, 1996, pp. 949–957; also NASA TM-106997, July 1995.

[5]Snyder, P. H., and Fish, R. E., "Assessment of a Wave Rotor Topped Demonstrator Gas Turbine Engine Concept," American Society of Mechanical Engineers, Paper 96-GT-041, June 1996.

[6]Paxson, D. E., "Recent Improvements to and Validation of the One Dimensional NASA Wave Rotor Model," NASA TM-106913, May 1995.

[7]Kentfield, J. A. C., *Nonsteady, One-Dimensional, Internal, Compressible Flows: Theory and Application*, Oxford Univ. Press, Oxford, England, UK, 1993.

[8]Azoury, P. H., *Engineering Applications of Unsteady Fluid Flow*, Wiley, New York, 1992.

[9]Paxson, D. E., "A General Numerical Model for Wave Rotor Analysis," NASA TM-105740, July 1992.

[10]Welch, G. E., "Two-Dimensional Computational Model for Wave Rotor Flow Dynamics," *Journal of Engineering for Gas Turbines and Power*, Vol. 119, No. 4, 1997, pp. 978–985; also NASA TM 107192, June 1996.

[11]Larosiliere, L. M., "Wave Rotor Charging Process: Effects of Gradual Opening and Rotation," *Journal of Propulsion and Power*, Vol. 11, No. 1, 1995, pp. 178–184.

[12]Paxson, D. E., "A Comparison Between Numerically Modelled and Experimentally Measured Loss Mechanisms in Wave Rotors," AIAA Paper 93-2522, 1993; also NASA TM-106279, June 1993.